Upgrade of the BioMUR beamline at the Kurchatov synchrotron radiation source for serial small-angle X-ray scattering experiments in solutions

Peters G.S.[1], Gaponov Yu.A.[1], Konarev P.V.[1,2], Marchenkova M.A.[1,2], Ilina K.B[1,2], Volkov V.V.[2], Pisarevsky Yu.V.[1,2], and Kovalchuk M.V.[1,2]

[1]*National Research Centre "Kurchatov Institute", Akademika Kurchatova pl., 1, Moscow, 123182, Russian Federation*

[2]*A.V.Shubnikov Institute of Crystallography of Federal Scientific Research Centre"Crystallography and Photonics" of Russian Academy of Sciences, Leninskii pr. 59, Moscow, 119333, Russian Federation*

E-mail: georgspeters@gmail.com

Abstract

Technical and methodological work was carried out to improve the quality of the experiments at the small-angle X-ray scattering (SAXS) beamline "BioMUR" at the Kurchatov synchrotron radiation source, commissioned in 2018. Scatterless slits (JJ X-Ray company, Denmark) were installed and tested, and the beam adjustment scheme of the "BioMUR" modified accordingly. Now outdated and not very effective mylar windows were replaced by mica vacuum windows providing significantly lower parasitic scattering. SAXS experiments on the solutions of weakly scattering lysozyme and bovine serum albumin proteins confirmed the significant improvement in the signal-to-noise ratio achieved due to the upgrade of the "BioMUR".

Keywords: synchrotron, optics, beamline, X-ray, scattering, upgrade

1. Introduction

The small-angle X-ray scattering (SAXS) beamline "BioMUR" at the Kurchatov synchrotron radiation source commenced operation in 2018 [1] and many user groups have successfully performed SAXS experiments on the beamline. In particular, good quality scattering data has been collected for the study of the oligomeric composition of crystallization solutions of potassium dihydrogen phosphate (KDP) [2] and transaminase from the thermophilic bacterium *Thermobaculum terrenum* [3], and the low-resolution three-dimensional structures of various aptamers in complex with proteins and DNA in solution were reconstructed [4]. Reliability of the obtained results was confirmed by independent experimental methods, but the quality and convenience of the experiment were far from optimal.

The initial experiments performed at the BioMUR beamline required accurate sample handling and manipulation of weakly scattering solutions of biomolecules. Beamline scientist noticed that users usually prepare a range of low-concentration samples and vary sample conditions (eg. pH, ionic strength, buffer composition) such that maintaining a stable background with minimal parasitic scattering is challenging. Within the framework of a single experiment, it is required to conduct several similar measurements, changing only the sample under study, while in order to ensure the adequate background subtraction from the experimental SAXS curves, the beam must be stable both at the sample position and at the detector throughout the entire period of the experiment.

These challenges have been successfully overcome at many SAXS synchrotron beamlines worldwide. It is clear that the quality of the data acquired is significantly affected by the presence of parasitic scattering from collimation slits [5]. To eliminate this deleterious scattering the most popular approach is to replace one or two blocks of standard slits in a three-slit collimation scheme with so-called "scatterless slits" – this was done, for example, at the P12 beamline (PETRA III, Germany) [6] and at the BL-6A beamline (Photon Factory, Japan) [7]. The edges of the scatterless slits are made of single crystals oriented at such angles that the incident X-rays are diffracted rather than scattered/reflected [8]. Such designs are offered, in particular, by Xenocs (France) and JJ X-Ray (Denmark).

Moreover, it is also extremely important to choose the material of the windows separating the vacuum between the experimental setup and the in-air sample environment, since they can produce a very significant contribution to the final scattering pattern. The tests of various materials of vacuum windows using SAXS are described in [9]. In principle, on SAXS beamlines, it is also possible to work without vacuum windows at all – as, for example, at the P12 beamline [6], but in this case, the sample must necessarily be placed in the common vacuum section of the setup, which is not always possible.

This paper describes the steps we have taken to improve the quality of SAXS experiments at the BioMUR beamline and presents the results of some SAXS experiments that clearly show the progress achieved.

2. Upgrade of the experimental setup

One of the main problems that remained after the commissioning of the "BioMUR" beamline was the presence of the beam scattering and reflection on the metal blades of the collimation slits. Moreover, this effect was especially pronounced in SAXS experimental modes, i.e., at sample-to-detector distances of 700 mm or more. This problem was exacerbated by small fluctuations of the synchrotron radiation beam around the established orbit due to the effects of stabilization in the storage device (in particular, the displacement of the beam due to the heating of the correctors over time and the subsequent return to the initial position). This resulted in a varying scattering intensity from the slit blades from exposure to exposure, as described in Fig. 1. Partly the reason for this was the design of the collimation slits at the beamline, the blades of which were made flat and unsharpened.

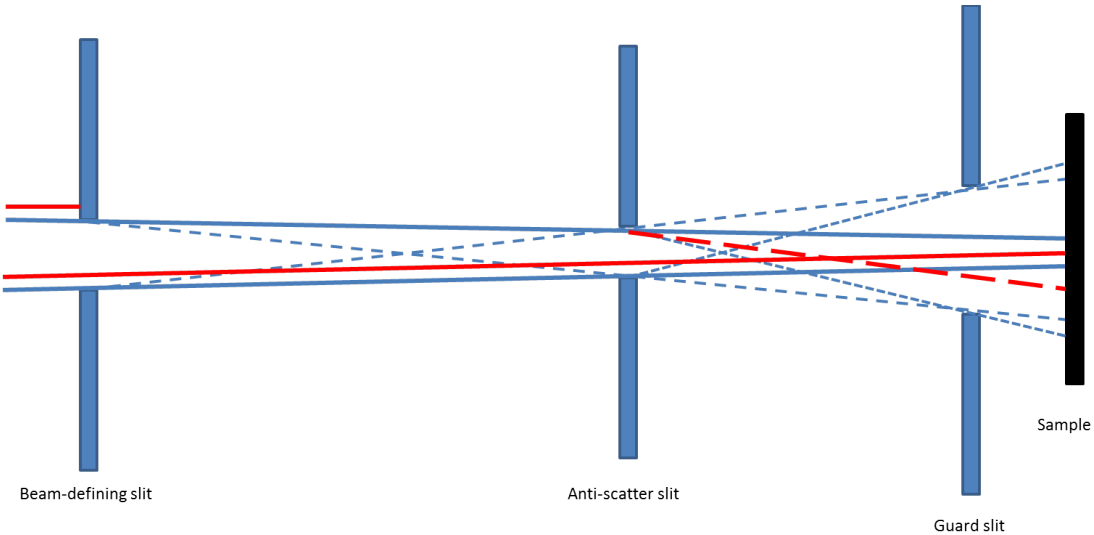

Fig. 1. Influence of the beam fluctuations on the parasitic scattering from the collimation slits, according to the standard three-slit collimation scheme [10]. Blue lines – normal beam position, red lines – non-stabilized position after beam fluctuations. The red dashed line indicates the strong reflections from the second slit flat blade resulting from the higher intensity unstablized beam.

Due to these facts, some experiments required many replicates, and the buffer solution was routinely measured multiple times. This was especially critical in case of weakly scattering protein solutions. To correct this situation, two sets of scatterless slits were purchased from JJ X-Ray, Denmark (Fig. 2, 3), which contain Si(110) crystals with a 90-degree cut and a thickness of 380 microns installed at the ends of tungsten carbide slit blades. The slit blades in the block are positioned apart in space to avoid their collision during movements.

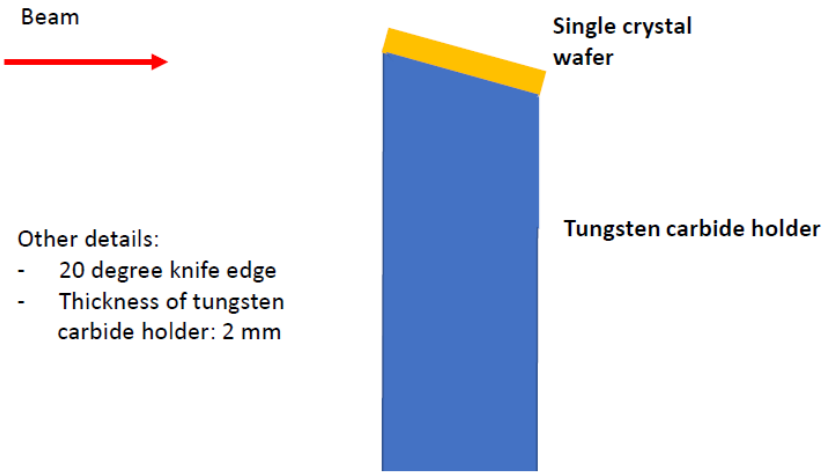

Fig. 2. Scheme and description of the JJ X-ray scatterless slits blade [8].

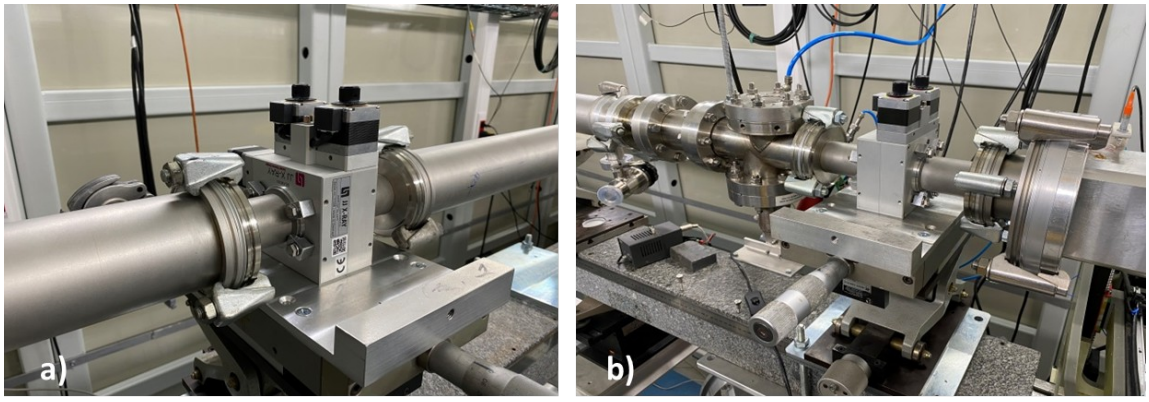

Fig. 3. Photos of the new scatterless slits installed at the “BioMUR” beamline – the anti-scatter slit (a) and the guard slit (b).

These scatterless slits replaced third and fourth blocks of standard slits, according to the notations of the old “BioMUR” setup [1] (second and third blocks in the traditional three-slit collimator scheme). As a result, the scattering from the slit blades was almost eliminated (Fig. 4). The fluctuations of the incident synchrotron radiation beam during the experiment ceased to affect the scattering intensity since the additional parasitic scattering from the collimator slits was effectively eliminated.

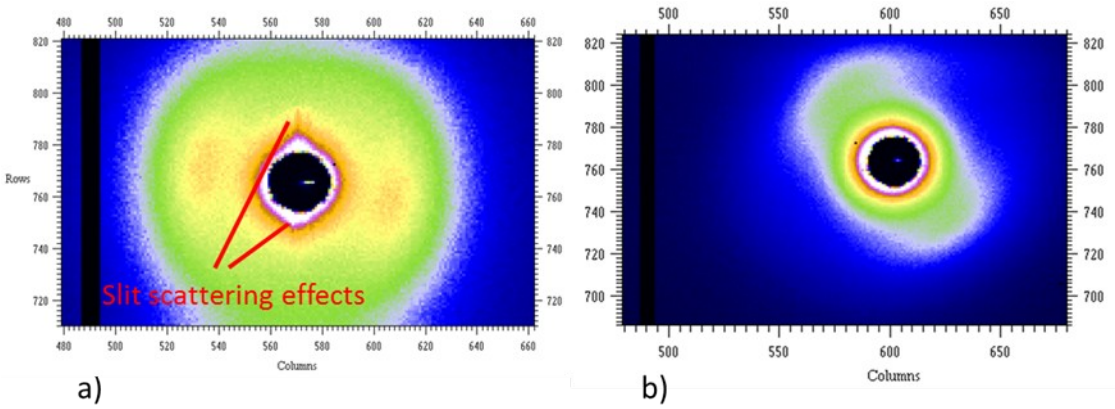

Fig. 4. Small-angle X-ray scattering in the vicinity of the beamstop: old conventional slits (a), new scatterless slits (b). Images obtained in Fit2D [11]

In addition to the improved characteristics of the beam at the sample, the procedure of the primary beam adjustment after the synchrotron radiation beam injection was significantly simplified and accelerated. Initially, after installation, the scatterless slits were adjusted to a certain "zero" position of the beam, at which the required energy of monochromatization and the angle of incidence on the mirror are fulfilled. During the experiment, the forward-scattered beam is usually intercepted by a beamstop. The new adjustment procedure consists of the following steps:

- An aluminum attenuating plate with a thickness of 500 microns is inserted into the beam;

- The beamstop is shifted beyond the beam limits (Fig. 5a) to observe the position of the direct beam relative to the slit positions;

- If necessary, the beam is returned to the “zero” position by changing the angles of inclination and rotation of the monochromator crystal (Fig. 5b);

- The beamstop is returned to the forward-scattered beam position, the attenuator is removed.

The main advantage of the new adjustment scheme is that the slit system tuning with the switched-on stabilization of the beam orbit is no longer required. The complete procedure began to take less than 5 minutes instead of 15-20 minutes required with the old scheme. The beam fluctuations associated with the stabilization effects of the beam orbit no longer require additional beam adjustment. As a result, a fully set up and centered beam remains always at the same position with fixed energy and angle of incidence, so no energy refinement is needed after the experiment.

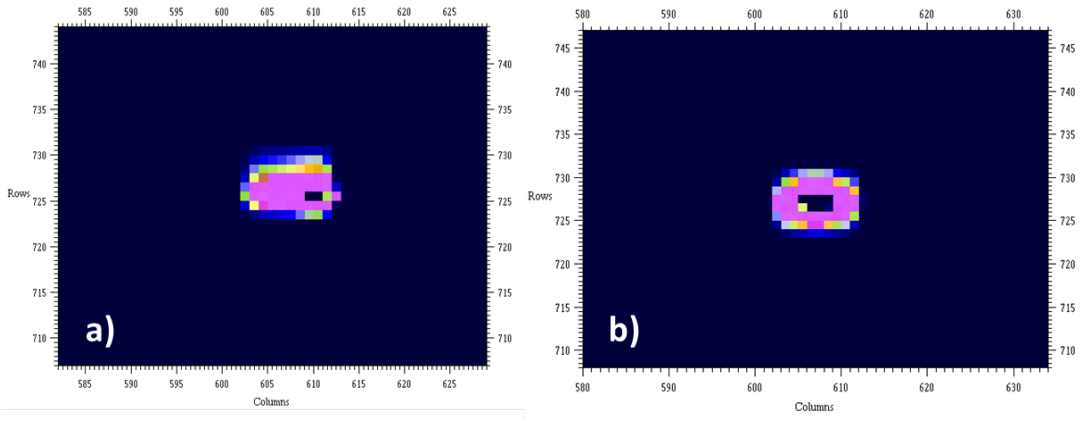

Fig. 5. Beam adjustment procedure: the removal of the beamstop and determination of the new beam position (a), return of the beam to the optimal position (b) with the attenuator installed. The beam size (FWHM) is 500x350 microns.

The second major challenge, as previously described in [1], was the selection of the appropriate material for the windows that separate the vacuum volumes from sample holder. The main factor limiting the choice of the material was the large aperture of the entrance window of the vacuum typesetting pipes, combined with the high level of vacuum in the span compartment with the installed collimation slits. During the initial operation of the beamline, it was observed that the scattering from the mylar windows makes a significant contribution to the acquired scattering pattern, comparable in magnitude to that from a low concentration protein solution. Therefore, to improve the quality and reliability of SAXS data, it was proposed to replace the entrance window in the vacuum tube of the span compartment. First of all, it was necessary to choose the most suitable material for window fabrication. For this purpose, SAXS measurements from films of various materials with a thickness of 9 to 220 microns were carried out on an automated laboratory source small-angle X-ray diffractometer "AMUR-K" (Moscow, Russia) [12], equipped with a one-dimensional position-sensitive gas detector OD3M at a fixed X-ray wavelength of 0.1542 nm (CuK_α is a line of the fine-focus X-ray tube, a monochromator is made of pyrolytic graphite) and Kratky collimation system (Fig. 6a). The X-ray beam cross-section was 0.2 x 8 mm, the angular range corresponded to the values of the scattering vector modulus $0.1 < s < 10.0$ nm^{-1}. The studied films were placed in a vacuum chamber. The sample-to-detector distance was 700 mm, the exposure time was 10 minutes.

High scattering signal at low angles was observed from films made of fluoroplast, polyethylene terephthalate, kapton, mylar, and polypropylene. Films made of a cycle-olefin copolymer were not completely amorphous, since they produced a wide diffraction peak in the region of $s \approx 1{,}0$ nm^{-1}, while a significant scattering in the region of low angles was also observed. Polylactide films had a low scattering signal, but due to their large thickness (90 microns), they absorbed strongly. Mica and polystyrene films had low scattering signals at low angles and absorbed weakly. Thus, the best X-ray characteristics were observed in films made of mica with a thickness of 40 microns and polystyrene with a thickness of 23 and 50 microns. However, for the entrance window of a vacuum pipe, a film with a size of at least 30 mm in each dimension was required. The linear dimensions of polystyrene films could not be larger than 20x30 mm for technological reasons, while mica films could be made up to 80x80 mm in size. As a result, mica films turned out to be the most suitable in size and X-ray characteristics for window fabrication.

Further, vacuum tests of mica windows were carried out at the Kurchatov Institute. In these tests, the size of the films varied from 10 to 80 mm and thickness varied from 20 to 100 microns. Unfortunately, these tests showed that the aperture of the entrance window must be reduced from 50 to a maximum of 25 mm, since films thinner than 40 microns and larger than 30 mm in diameter were destroyed by high vacuum, and thicker films have too high absorption. According to the test results, mica with a thickness of 40 microns was chosen as a material for the new vacuum windows, since 30 mm film could withstand a vacuum up to 10^{-6} mbar without any visible damage The comparison of the scattering curves from 15 microns of mylar and 40 microns of mica windows at the “BioMUR” beamline is shown in Fig. 6b. In this experiment, the sample-to-detector distance was 700 mm and the exposure time was 300 seconds.

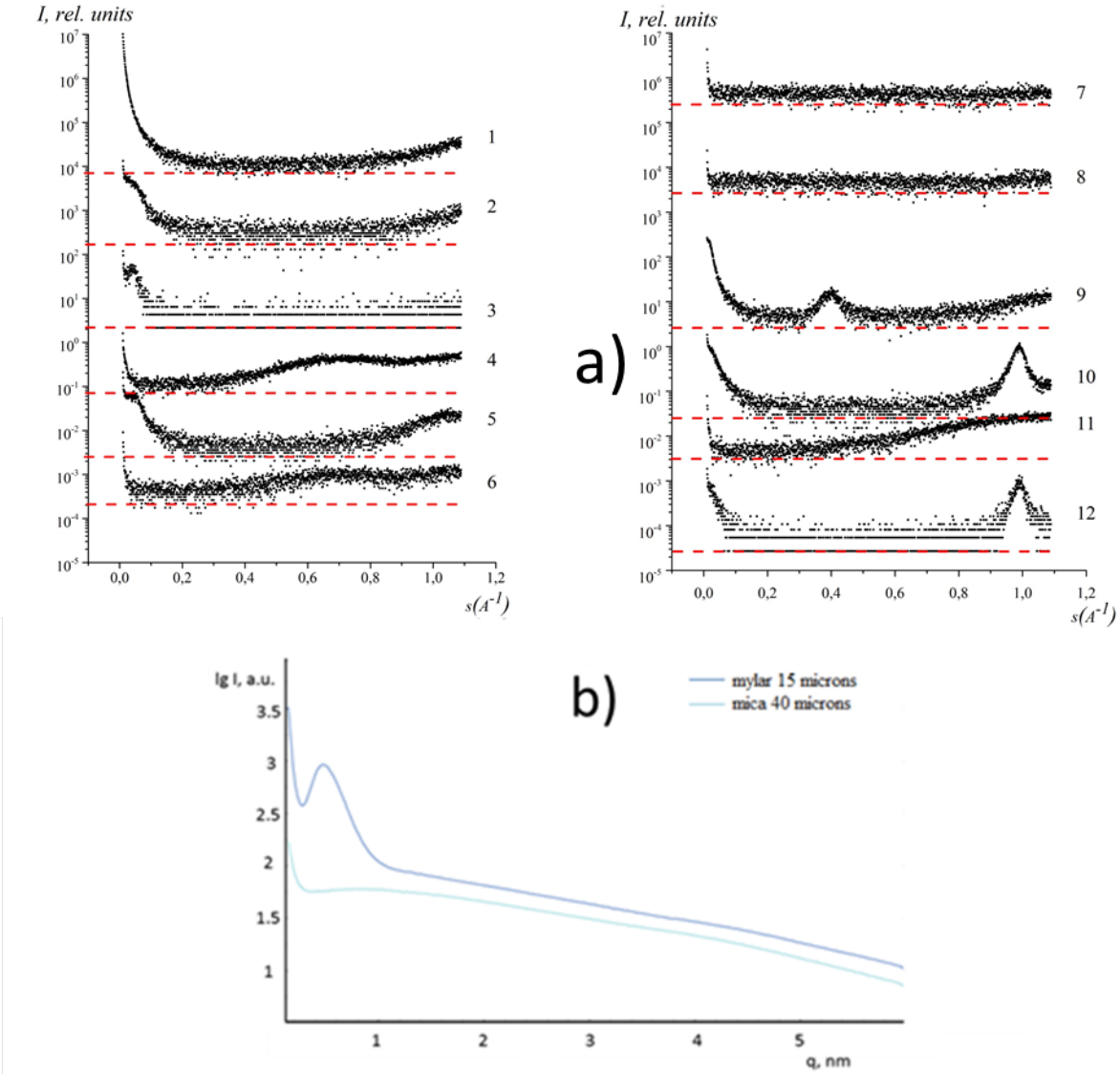

Fig. 6. Experimental SAXS curves of various materials obtained at the AMUR-K setup (a): 1. fluoroplast (the thickness is 9 microns); 2. polyethylene terephthalate (13 microns); 3. mylar (10 microns); 4. polystyrene (220 microns); 5. polystyrene (50 microns); 6. polystyrene (23 microns); 7. mica (40 microns); 8. mica for atomic-force microscopy (75 microns); 9. kapton (45 microns); 10. polypropylene (25 microns); 11. polylactide (90 microns); 12. cycle-olefin copolymer (50 microns). The curves are shifted vertically for better visualization, dashed lines indicate the level of zero intensity for each curve. (b) Comparison of the mica film (the material of the new vacuum window installed on the "BioMUR" beamline) with the mylar film (the material of the old vacuum window).

3. Experiments

After installing the new scatterless slits, the beam collimation of the experimental setup was further optimised. To verify the correct setting, a silver behenate powder for calibration of the angular axis of the instrument was measured. Figure 7 shows a comparison of the obtained scattering curve with a previous curve recorded with the old standard slits at the same sample-detector distance of 700 mm. Both curves were obtained by integrating the image in vertical projection Note, these experiments were carried out before the replacement of the vacuum windows.

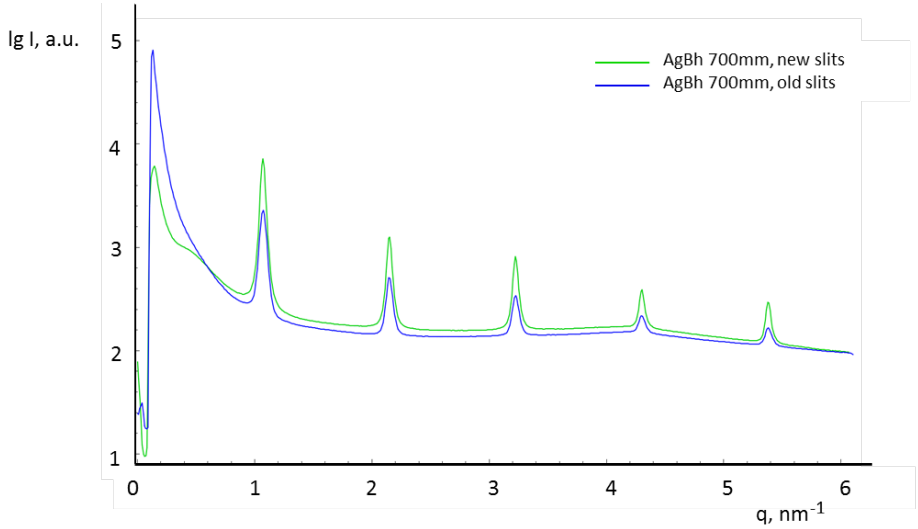

Fig. 7. Comparison of SAXS patterns of silver behenate before and after the replacement of collimation slits.

As a result, the curve quality had significantly improved due to the almost complete elimination of the background scattering on the collimation slits and become approximately 3.5 times better than with the old slits. Let I_{saxs} be the intensity maximum (near the beamstop) of overall SAXS scattering from the sample, which consists of contributions from AgBh, slits, kapton and vacuum windows, and I_{peak} – the intensity of AgBh first diffraction peak. We subtracted the baseline intensity from each value. Then, calculated from the curves, the old I_{peak}/I_{saxs} relation is 0.29 and the new value (after slit replacement) is 1.09 with the same AgBh sample. However, the artifacts associated with the parasitic scattering on vacuum windows, for the same reason, began to appear more pronounced. Obtained again from the curves, the old I_{wind}/I_{saxs} relation value is 0.11, where I_{wind} is the intensity of the scattering on vacuum windows only, and the new value is 0.27. This fact just confirmed the necessity of replacing the vacuum window material.

The first experiments with the new mica vacuum windows showed almost complete absence of their contribution to the scattering pattern from the protein. As an example, we present the SAXS curves from a lysozyme solution (molecular weight 14.3 kDa) at a protein concentration of 40 mg/ml (Fig. 8a), so that the scattering intensity is high enough to compare only the noise generated after subtraction of the buffer solution curve. As can be seen, the SAXS curve obtained with the old setup was distorted by strong parasitic scattering from the mylar window, and after its replacement with the mica window, almost "clean" SAXS data were obtained in the experiment.

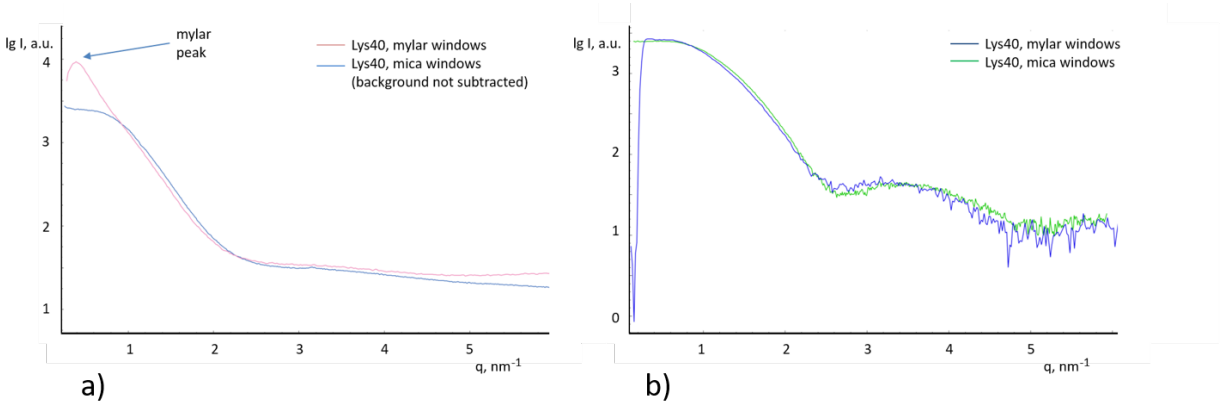

Fig. 8. Comparison of experimental SAXS curves from the solution of lysozyme protein (40 mg/ml) obtained with the old (mylar) and new (mica) vacuum windows - the initial curves (a) and the result of buffer subtraction (b). The exposure time in both cases was 180 seconds, the X-ray wavelength was 0.1445 nm, the sample-to-detector distance was 700 mm.

SAXS data collected following the beamline upgrade showed a significant reduction in noise, as can be seen from Figure 8b. This facilitated high-quality experiments using a two-fold reduction in the standard protein concentration required at the instrument. Thus, a previously hard to achieve high quality data set was acquired for the concentration series of solutions of bovine serum albumin (BSA) (molecular weight 66.4 kDa) (Fig. 9). Figure 9b shows that the BSA solution at 5 mg/ml still provides good scattering signal, which was not possible to obtain before the beamline upgrade. Table 1 displays the results of SAXS data analysis obtained with the help of the PRIMUS software (from the ATSAS program package) [13, 14] before and after the upgrade of the “BioMUR” beamline.

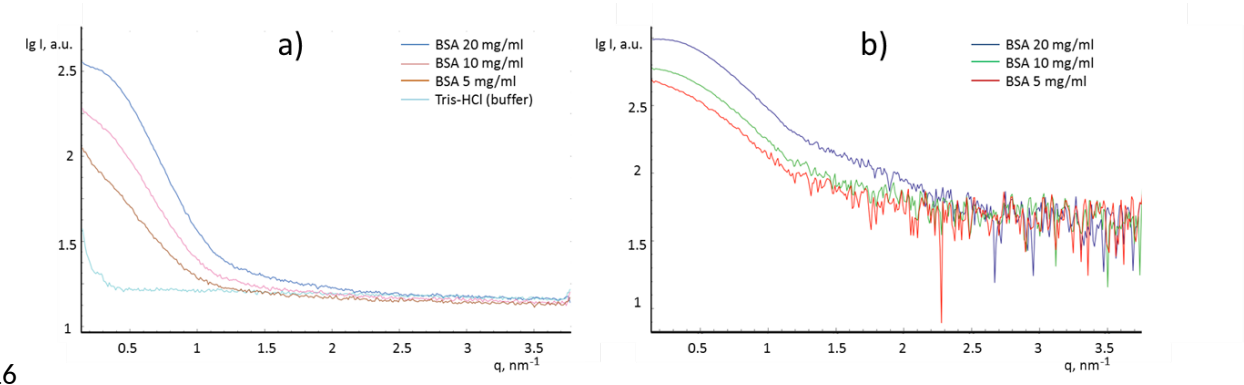

Fig. 9. Comparison of experimental SAXS curves from the BSA protein at different concentrations (20 mg/ml, 10 mg/ml and 5 mg/ml): before buffer subtraction (a), after buffer subtraction (b). The exposure time was 180 seconds, the X-ray wavelength was 0.1445 nm, the sample-to-detector distance was 700 mm.

Table 1. Comparison of SAXS structural parameters of lysozyme and BSA proteins obtained before and after the upgrade of the “BioMUR” beamline.

Sample	Beamline conditions	Conc, mg/ml	R_g (Guinier), nm	R_g (from p(r)), nm	Total quality estimate parameter from GNOM [15]
Lysozyme	before upgrade	40.0	1.46±0.02	1.49±0.03	0.58
Lysozyme	*after upgrade*	*40.0*	*1.35±0.01*	*1.37±0.02*	*0.67*
BSA	before upgrade	20.0	2.86±0.05	2.81±0.05	0.55
BSA	*after upgrade*	*20.0*	*2.80±0.03*	*2.82±0.03*	*0.65*
BSA	*after upgrade*	*10.0*	*2.81±0.03*	*2.85±0.05*	*0.63*
BSA	*after upgrade*	*5.0*	*2.96±0.03*	*2.95±0.03*	*0.58*

*R_g denotes the radius of gyration of the protein molecule

4. Conclusions

Upgrading X-ray instrumentation through the installation of scatterless slits and using vacuum sealed mica windows is a relatively inexpensive procedure. As a result of the work on improving and optimizing the optical elements at the “BioMUR” beamline, it was possible to deliver a high intensity X-ray beam almost free from parasitic scattering coming from the collimation system.

In addition, SAXS patterns from protein solutions having three times higher signal-to-noise ratio compared to the original beamline configuration can now be routinely collected. The sensitivity of the beamline was also increased when measuring protein solutions at low concentrations, which is especially important for experiments conducted on weakly scattering biomolecules and systems prone to aggregate. Finally, due to the replacement of the standard collimation slits with a scatterless system and optimization of the slit adjustment procedure, it was possible to significantly reduce the beamline tuning time and the "dead" time between exposures by a factor of two. The serial SAXS experiments with the proteins in solutions have therefore become possible to conduct with high accuracy.

5. Acknowledgements

The authors acknowledge A. S. Khlebnikov (Kurchatov Institute, Moscow) for the assistance in installation of the new optical elements and organization of the technical work, A.A. Veligzhanin (Kurchatov Institute, Moscow) for the methodological advice, as well as Dr. H.D.T. Mertens (EMBL, Hamburg Outstation, Germany) for his help in preparing the English version of the manuscript. The upgraded “BioMUR” beamline is a part of the unique scientific facility Kurchatov Synchrotron Radiation Source supported by the Ministry of Science and Higher Education of the Russian Federation (project code RFMEFI61917X0007). The reported study was supported by RFBR according to the research project № 19-29-12042 mk and by the Ministry of Science and Higher Education within the State assignment FSRC ‘‘Crystallography and Photonics’’ of Russian Academy of Sciences (RAS) (SAXS analysis). SAXS measurements of films for materials of vacuum windows were performed using the equipment of the Shared Research Center FSRC “Crystallography and Photonics” of the Russian Academy of Sciences and were supported by the Ministry of Science and Higher Education of the Russian Federation (project RFMEFI62119X0035).

Literature

[1] Peters, G. S., Zakharchenko, O. A., Konarev, P. V., Karmazikov, Y. V., Smirnov, M. A., Zabelin, A. V., Mukhamedzhanov, E.H., Veligzhanin, A.A., Blagov, A.E., Kovalchuk, M. V. (2019). The small-angle X-ray scattering beamline BioMUR at the Kurchatov synchrotron radiation source. Nuclear Instruments and Methods in Physics Research Section A: Accelerators, Spectrometers, Detectors and Associated Equipment 945, 162616.

[2] Kovalchuk, M.V., Alekseeva, O.A., Blagov, A.E., Ilyushin, G.D., Il'ina, K.B., Konarev, P.V., Lomonov, V.A., Pisarievsky Yu. V., Peters, G. S. (2019). Investigation of the Structure of Crystal-Forming Solutions of Potassium Dihydrogen Phosphate K (H 2 PO 4) (KDP type) on the Basis of Modeling Precursor Clusters and According to Small-Angle X-Ray Scattering Data. Crystallography Reports 64, 6-10.

[3] Marchenkova, M.A., Konarev, P.V., Rakitina, T.V., Timofeev, V.I., Boikova, A.S., Dyakova, Y.A., Ilina, K.B., Korzhenevskiy, D.A., Yu Nikolaeva, A., Pisarevsky, Y.V., Kovalchuk, M.V. (2020) Journal of Biomolecular Structure and Dynamics 38, 2939-2944.

[4] Tomilin, F.N., Moryachkov, R., Shchugoreva, I., Zabluda, V.N., Peters, G., Platunov, M., Spiridonova, V., Melnichuk, A., Atrokhova, A., Zamay, S., Ovchinnikov, S., Zamay, G.S., Sokolov, A., Zamay, T., Berezovski, M., Kichkailo, A.S. (2019). Four steps for revealing and adjusting the 3D structure of aptamers in solution by small-angle X-ray scattering and computer simulation. Analytical and bioanalytical chemistry 411, 6723-6732.

[5] Kirby, N. M., Mudie, S. T., Hawley, A. M., Cookson, D. J., Mertens, H. D., Cowieson, N., Samardzic-Boban, V. (2013). A low-background-intensity focusing small-angle X-ray scattering undulator beamline. Journal of Applied Crystallography 46, 1670-1680.

[6] Blanchet, C. E., Spilotros, A., Schwemmer, F., Graewert, M. A., Kikhney, A., Jeffries, C. M., Franke, D., Mark, D., Zengerle, R., Cipriani, F., Fiedler, S., Roessle, M., Svergun, D. I. (2015). Versatile sample environments and automation for biological solution X-ray scattering experiments at the P12 beamline (PETRA III, DESY). Journal of Applied Crystallography, 48, 431-443.

[7] Shimizu, N., Mori, T., Igarashi, N., Ohta, H., Nagatani, Y., Kosuge, T., Ito, K. (2013). Refurbishing of small-angle X-ray scattering beamline, BL-6A at the photon factory. Journal of Physics: Conference Series 425, 202008.

[8] Li, Y., Beck, R., Huang, T., Choi, M.C., & Divinagraci, M. (2008) Scatterless hybrid metal–single-crystal slit for small-angle X-ray scattering and high-resolution X-ray diffraction. Journal of Applied Crystallography 41, 1134–1139.

[9] Masunaga, H., Sakurai, K., Akiba, I., Ito, K., & Takata, M. (2013). Accurate measurements of intrinsic scattering from window materials by use of a vacuum camera. Journal of Applied Crystallography 46, 577-579.

[10] Glatter, O. Kratky, O. Small Angle X-Ray Scattering, Academic press, 1982.

[11] Hammersley, A.P. (2016). FIT2D: a multi-purpose data reduction, analysis and visualization program. Journal of Applied Crystallography 49, 646-652.

[12] Mogilevskiy, L.Y., Dembo, A.T., Svergun, D.I., Feygin, L.A. (1984). Small-angle X-ray diffractometer with single coordinate detector. Crystallography Reports 29, 587-591.

[13] Konarev, P.V., Volkov, V.V., Sokolova, A.V., Koch, M.H.J., Svergun, D.I. (2003). PRIMUS - a Windows-PC based system for small-angle scattering data analysis. Journal of Applied Crystallography 36, 1277-1282.

[14] Manalastas-Cantos, K., Konarev, P.V., Hajizadeh, N.R., Kikhney, A.G., Petoukhov, M.V., Molodenskiy, D.S., Panjkovich, A., Mertens, H.D.T., Gruzinov, A., Borges, C., Jeffries, C.M., Svergun, D.I., Franke D. (2021). ATSAS 3.0: expanded functionality and new tools for small-angle scattering data analysis. Journal of Applied Crystallography 54, 343-355.

[15] Svergun, D.I. (1992). Determination of the regularization parameter in indirect-transform methods using perceptual criteria. Journal of Applied Crystallography 25, 495-503.